

How to detect Berry phase in graphene without magnetic field?

Hamed Koochaki Kelardeh*, Vadym Apalkov, Mark I. Stockman
Center for Nano-Optics (CeNO) and Department of Physics and Astronomy
Georgia State University, Atlanta, GA

Abstract

We discuss the topological properties of graphene superlattices excited by ultrafast circularly-polarized laser pulses with strong electric field amplitude, aiming to directly observe the Berry phase, a geometric quantum phase encoded in the graphene's electronic wave function. As a continuing research on our recent paper, Phys. Rev. B 96, 075409, we aim to show that the broken symmetry system of graphene superlattice and the Bragg reflection of electrons creates diffraction and "which way" interference in the reciprocal space reducing the geometrical phase shift and making it directly observable in the electron interferograms. Such a topological phase shift acquired by a carrier moving along a closed path of crystallographic wave vector is predictably observable via time and angle-resolved photoemission spectroscopy (tr-ARPES). We believe that our result is an essential step in the control and observation of ultrafast electron dynamics in topological solids and may open up a route to all-optical switching, ultrafast memories, and petahertz-scale information processing technologies.

Keywords: Ultrafast optics, 2D Dirac materials, Berry phase, tr-ARPES

1. INTRODUCTION

The development of ultrafast lasers with controllable carrier-envelope phase (CEP) able to generate sub-10 fs optical pulses and has made optical control of condensed matter systems and coherent electron dynamics especially appealing [1-7]. It also provides a testbed for the realization of features and properties that were hardly attainable a decade ago. The topological nature of materials is among the most important characteristics that have intrigued people for some time, but their control and manipulation have come to a new perspective on the development of attosecond science. Quantum mechanical systems undergoing adiabatic evolution on a closed path in the Hilbert space acquire a topological

^{0*} hkelardeh@physics.gsu.edu

phase known as Berry's phase [8-10]. In condensed matter physics, the Berry flux and its density, i.e., Berry curvature, in the momentum space play a key role in the emergence of unique phenomena such as the anomalous [11] and quantum [12] Hall effects, and topological insulating and superconducting phases [13]. Graphene as the building block of two-dimensional nanosystems exhibits fascinating properties such as high carrier mobility [14, 15], exceptional optoelectronic behavior [16], and unconventional room-temperature quantum Hall effect. Such phenomena make graphene a promising platform for engineering ultrafast devices and all-carbon nanoelectronics. Close to the Fermi level, the energy spectrum of graphene varies linearly with its momentum, and the dynamics of electrons resembles the two-dimensional gas of Massless Dirac Fermion (MDF) with a speed of 0.01 speed of light. The coupling of graphene electrons to the incoming light is strong and due to the gapless energy dispersion, the response time of electron and photon interaction is known to be ~ 10 as [17, 18], which is an order of magnitude faster than the responsivity of bound electrons in atomic, molecular and semiconducting solids [19]. Indeed, the zero band gap in graphene makes it intriguing because in principle, we have resonance electron dynamics at large spectrum from THz all the way to UV frequencies.

It has been known for a long time that if the energy dispersion near a degenerate point is linear, then the cyclotron orbit will acquire a π -Berry phase, independent of the shape of the orbit [20]. However, the Berry phase, as a fundamental topological attribute, has never been directly observed in real graphene. The indirect demonstration of the Berry phase has been experimentally observed via a quantum Hall plateau at zero energy [21, 22]. In the same way, in the previously published research [23] and [24], the Berry phase is implicitly observed through an angular dependence of the interband matrix elements in graphene, related to a specific structure of the electron wave function defined by the crystallographic symmetry.

The explicit indication of Berry's phase, though, requires moving electrons around the Dirac point. In our previous work [25], we proposed an ultrafast interferometric technique with the use of a two-cycle circularly polarized pulse aiming to directly determine the Berry phase shift in the excitation map of electron dynamics. Although we see a sharp jump in the real and imaginary components of the electron wave function, the probability amplitude as a measurable quantity is blind to such a phase shift. However, the Berry phase shows its signature with the presence of an extra fringe and the appearance of bifurcation in the conduction band population distribution - see Fig. 2 in Ref. [25] and its discussion.

In this paper, we propose the solution to a fundamental problem of directly observing the Berry phase in the graphene reciprocal space which will open up a new route in controllable light-driven electronic devices and hold promises in various applications such as ultrafast memories, petahertz data processing, and room temperature superconductivity. We show that graphene deposited on the hexagonal Boron Nitride (h-BN), by breaking the inversion symmetry can reduce the symmetry of the system and allow us to directly see the Berry phase and its corresponding jump in the conduction band population distribution. The

fabrication process of Graphene on h-BN sometimes referred to as the insulating counterpart of graphene due to their matching hexagonal structures, results in the formation of a topographic moiré pattern [26-30]. This moiré pattern produces a weak periodic potential that causes the Berry phase to be different from $\pm\pi$ and allows it to directly manifest in the excitation distribution of electrons in graphene. As an alternative, such a periodic modulation of electronic potential can be attained by using an array of nanowires under electrostatic bias superimposed beneath the graphene monolayer with a well-defined spatial periodicity [31]. Our proposed theory and the population distribution induced by the strong optical field in the reciprocal space can be verified by time- and angle resolved photoemission spectroscopy (tr-ARPES) techniques.

2. MODEL DESCRIPTION

In our theory, we use the tight binding model of graphene with the two-band electron system, i.e., a conduction band (CB) and a valence band (VB). Our non-magnetic optical pulse is a single-cycle with vacuum wavelength $1.5\mu\text{ m}$ and a pulse duration of 5 femtoseconds. The electric field vector of the laser, \mathbf{F}_L , has components in the plane of graphene as:

$$F_x(t) = -F_0 e^{-t^2} (1 - 2t^2), \quad F_y(t) = \pm 2t F_0 e^{-t^2} \quad (1)$$

where \pm signs correspond to the right and left polarized pulse. F_0 the amplitude of the pulse is related to its power, \mathcal{P} , through the relationship $\mathcal{P} = cF_0^2/4\pi$. If the pulse duration is less than the characteristic scattering time, then the electron dynamics become coherent. In this case, the scattering processes during pulse propagation (including electron-electron collisions), do not have the time to produce a significant effect on the electron dynamics [32-40]. The excitation dynamics of electrons in graphene interacting with the ultrafast optical field in the coherent regime is described by the time-dependent Schrödinger equation (TDSE):

$$i\hbar \frac{d\Psi(t)}{dt} = \mathbf{H}(t)\Psi(t) \quad (2)$$

with the general Hamiltonian of the closed system as

$$\hat{\mathbf{H}} = \hat{\mathbf{H}}_0 + e\mathbf{F}_L(t) \cdot \mathbf{r} + V \cos(\mathbf{Q} \cdot \mathbf{r})\hat{\mathbf{I}} \quad (3)$$

where $\hat{\mathbf{H}}_0$ is the field-free Hamiltonian of graphene described by the tight-binding (TB) model with nearest neighbor hopping, \mathbf{r} is the planar vector of monolayer graphene and $\hat{\mathbf{I}}$ is the identity matrix. $\mathbf{Q} = \{0, Q_y, 0\}$ with $Q_y = 2\pi/L$ is the reciprocal superlattice vector corresponding to the periodic potential generated by the h-BN substrate. The pulse's external, time-dependent electric field of the pulse has an impact on electronic motion, that is, the field induces electron motion within a single band (interband dynamics) and induces the coupling of electron states of different bands (interband dynamics). Such

interband coupling is similar to Zener interband tunneling in constant, external electric fields [41, 42].

We neglect the spin-orbit interaction, which is known to be negligibly small ($\sim 1\mu\text{eV}$) in graphene [43]. Within a single band, the dynamics of an electron in momentum (wave vector) space is appropriately described by the Houston function. At the initial moment of time, i.e., before the pulse, the Houston function is the Bloch function with wave vector \mathbf{k}_0 .

With time, the electron wave vector is shifted by the value $\Delta\mathbf{k}(t) = \mathbf{k}(t) - \mathbf{k}_0 = \frac{e}{\hbar} \int_{-\infty}^t \mathbf{F}_L(t') dt'$, which is independent of the initial wave vector, \mathbf{k}_0 . Therefore, within a single band, the electron dynamics in the reciprocal space are described by the Bloch acceleration theorem $\frac{d\mathbf{k}(t)}{dt} = \frac{e}{\hbar} \mathbf{F}_L(t)$ which is universal and is valid for any dispersion relation [44].

The states that belong to different bands (VB and CB) but have the same initial crystal wave vector, \mathbf{k}_0 , will have the same crystallographic wave vector, $\mathbf{k}(t)$, at all moments of time t . After the pulse ends, the wave vector returns to its initial value \mathbf{k}_0 . The periodic potential coming from the moiré superlattice couples states within each band with crystal moments \mathbf{k} and $\mathbf{k}' = \mathbf{k} \pm n\mathbf{Q}$, where $n = \pm 1, \pm 3, \dots$ is the order of the Bragg reflection from the underlying h-BN substrate. Assuming potential $\Delta(y)$ to be smooth and weak enough, we will only take into account $n = \pm 1$.

In Fig. 1 we illustrate and graphically explain our graphene superlattice proposal: Panel (a) represents the schematic of the interaction process of the few-cycle circular pulse with the graphene superlattice created by superimposing it on the hBN. In panel (b) the band structure including the highest VB, the lowest CB, and the Dirac points, K and K', are shown. Panel (c) shows an electron trajectory (the dashed red line) for an isolated monolayer of graphene in the reciprocal space caused by a single-oscillation circularly polarized pulse. The separatrix (shown by the solid blue line) is the position of initial wave vectors where their corresponding trajectories pass precisely through the Dirac point [45]. If the initial point, \mathbf{k}_0 , is outside of the separatrix, as in panel (c), then the trajectory does not encircle the Dirac point, and the total Berry phase accumulated on such a trajectory is zero. In contrast, if \mathbf{k}_0 is inside the separatrix, as in panel (d), then the trajectory encircles the Dirac point and, consequently, the Berry phase is $\pm\pi$ for the K - and K' point, respectively. Panel (e) shows the electron trajectory for the graphene superlattice; the red line shows the actual electron trajectory in the reciprocal space starting at a crystal wave vector \mathbf{k}_0 , where the solid line corresponds to the electron in the VB and the dashed line in the CB. There are also two additional trajectories shown by the dash-dot blue and green lines that are obtained from the original (red) trajectory by shifting it with the superlattice reciprocal vectors, $\pm\mathbf{Q}_y$. The electron moving along the original (red) trajectory undergoes a Bragg reflection from the superlattice acquiring the wavevector $-\mathbf{Q}_y$ and jumps to the blue trajectory, as shown by a vertical arrow. This jump is necessarily accompanied by a VB \rightarrow CB transition to avoid the Pauli blocking due to the VB being fully occupied. Passing by the K' - point, the electron undergoes the CB \rightarrow VB

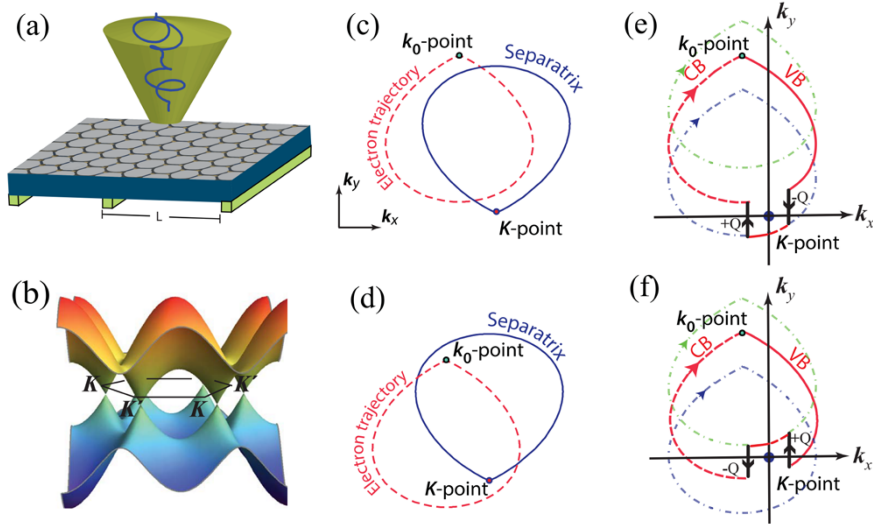


Figure 1: (a) Schematic of the proposed structure. A graphene monolayer is positioned over a superlattice formed by nanowires with period L and gating potential V (or analogously deposited on a h-BN substrate which produces the so-called moiré pattern with a well-defined superlattice wavelength L and potential strength V). Inset: Illustration of the electric field waveform $\mathbf{F}(t) = \{F_x(t), F_y(t)\}$ as a function of time t for a single oscillation circularly polarized ultrashort pulse. (b) Electron dispersion of graphene monolayer obtained within tight-binding approximation. Energies of the highest valence band (π -band) and the lowest conduction band (π^* -band) in the reciprocal space are displayed as functions of wavevector $\mathbf{k} = \{k_x, k_y\}$. The two distinct Dirac points are labeled as K and K' . (c) An illustration of an electron trajectory (dashed red line) in the reciprocal space, which starts and ends at a \mathbf{k}_0 -point outside the separatrix and passes close to the K -point without circling it. The separatrix (solid blue line) separates the \mathbf{k}_0 -points for those trajectories that circle the K -point and those that do not. (d) The same as in panel (c) but for the \mathbf{k}_0 point inside the separatrix. (e) Schematic of the reciprocal space trajectories and transitions caused by the Bragg reflections for the \mathbf{k}_0 -point outside of the separatrix, corresponding to the case of the panel (c). The red line shows an electron trajectory where the solid and dashed segments correspond to the VB and CB, respectively, as indicated. The thin dash-dot green and blue lines are Bragg-shifted replicas of the original trajectory. (f) The same as in panel (e) but for the \mathbf{k}_0 -point inside the separatrix, corresponding to the case of the panel (d).

transition and then another $VB \rightarrow CB$ transition at the point of the second Bragg reflection. The electron completes its trajectory at the initial \mathbf{k}_0 point but in the CB state. In both cases of the initial crystal moments inside and outside of the separatrix [Fig. 1 (e)-(f)], the electron circles the K - point but only in part, hence the accumulated Berry phase along the passage is less than π and makes it observable as sharp phase jumps in the reciprocal space carrier distribution - see Fig. 2 and 3.

The further derivation and computation procedure is elaborated in Ref. [31]. In the next section, we present some results of numerical solutions for graphene interacting with the circular pulse. We show that the deposition of graphene on substrates breaks the fundamental lattice symmetries and by changing the electronic spectrum of graphene, leads to the manifestation of the Berry phase as well as interesting signatures of valley polarization and generation of Hall current perpendicular to the drift current induced by the electric field of the pulse.

3. RESULTS AND DISCUSSION

To elucidate the topological Berry phase corresponding to the electronic states of graphene at the Dirac points, we turn to Figs 2 and 3 where the residual population of conduction-band states is illustrated with the false color. Fig. 2 shows the results of our two-band model for graphene interacting with a single cycle circularly polarized pulse with field strengths ranging from 0.25 to 1 V/Å. The simulation has been illustrated in the extended Brillouin zone (BZ) for better comprehension. We employed the realistic values [26] for both the potential strength and the moiré wavelength; $V=0.05$ eV, and $L = 10$ nm. The discontinuity in the population distribution of the reciprocal space corresponding to the Berry phase is apparent.

Due to the intrinsic chirality of graphene, as the field amplitude increases, the interaction and population exchange between K and K' valleys increases. In principle, the separatrix governs the trajectory of the electron wave packet around the K and K' points. A higher field means larger separatrix; when the trajectory around one Dirac point gets sizable such that it passes in the region of the neighboring Dirac point, there will be a proximity area where the two Quantum pathways with different directionality and phase properties start to overlap with each other. This partial intersection produces the interference fringes that are observable for the field amplitudes of 0.75 and 1 V/Å in Fig. 2 and 3.

A subtle, yet interesting feature of the population distribution with the use of a circularly polarized pulse is that the superlattice potential induced by the h-BN substrate breaks the inversion symmetry of the graphene system giving rise to the population imbalance in the nonequivalent K and K' valleys and the manifestation of the quantum Valley Hall Effect (QVHE) [46, 47]. One can note the presence of valley Hall current as a consequence of opposite Berry curvature at K and K' , by the significant difference in the carrier distribution around

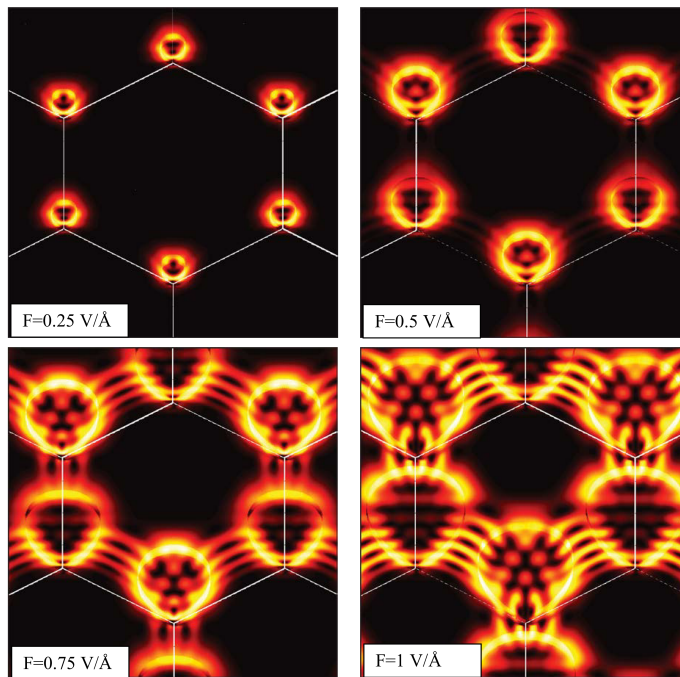


Figure 2: The CB population distribution in the extended BZ scheme for a single-cycle circularly polarized field after the end of the excitation pulse whose amplitudes are (a) $F_0 = 0.5$, (b) 0.5, (c) 0.75 and (d) 1 V/Å, respectively. The distributions of the population in the vicinity of the K - vs. K'-point are different because the chirality of the circularly-polarized pulse causes significantly different electron trajectories at the nonequivalent Dirac points, which are intrinsically chiral themselves. (Note that for linearly polarized pulses, there is no such a distinction: the distribution at the K - and K'-points are identical - see Ref. [18].

nonequivalent valleys.

Another important attribute one may infer by analyzing the CB population distribution of graphene is the possibility of Valley polarization in graphene. The valley degeneracy at K and K' Dirac points in the momentum space present an additional degree of freedom for charge carrier manipulation. Analogous to the spin states in spintronics, controlling the population of valley states is essential to the development of valley-based devices with graphene and other topological two-dimensional materials. The circularly polarized pulse lifts such degeneracy in a controlled way and reveals the chiral nature of graphene.

Degeneracy lifting of the valley degree of freedom is directly related to the global sublattice symmetry breaking. We cannot distinguish the nonequivalent Dirac points of graphene's band structure with the linear pulse since it is achi-

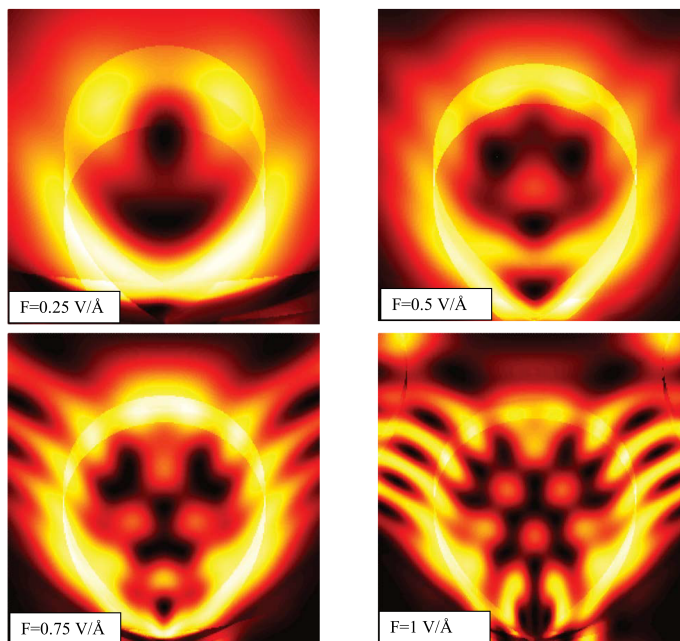


Figure 3: The CB population distribution around the K-point to visualize the phase shift accompanied by the nontrivial Berry phase of graphene’s electronic wave function. As the field amplitude increases, the carrier distribution around the K-point starts to intersect with its neighboring Dirac point and introduces interference fringes.

ral and a superposition of right and left circularly polarized pulse. In a sense, the effect of the Berry phase in reciprocal space is in correspondence with the Aharonov-Bohm effect in the configuration space where a phase is acquired if the electrons diffract moving around the magnetic flux [48]. In fact, the Dirac point in graphene has a local Berry flux that acts like a local magnetic field.

To better visualize the discontinuities at the separatrices and their Bragg replica, corresponding to the Berry phase, here we pinpoint the excitation distribution of the CB states to enclose only the K- Dirac point. The three discontinuities are clearly seen at the separatrix and its replicas Bragg-shifted by $\pm\mathbf{Q}$. The interference fringes of population dynamics and the discontinuity corresponding to the topological Berry phase are observable using tr-ARPES. The electron-electron collision dynamics will manifest itself by the smearing-out of the interferograms, which can also be traced by TRARPES with a temporal resolutions of a few fs and the momentum resolution defined by the ARPES setup, which is realistically ~ 1.5 percent of the Brillouin zone edge ($\approx 1.6\text{\AA}$) that is $\approx 0.025\text{\AA}$ [49]; the momentum resolution can be as high as 0.005\AA for nano-ARPES [50]. Such resolutions are more than sufficient to observe the in-

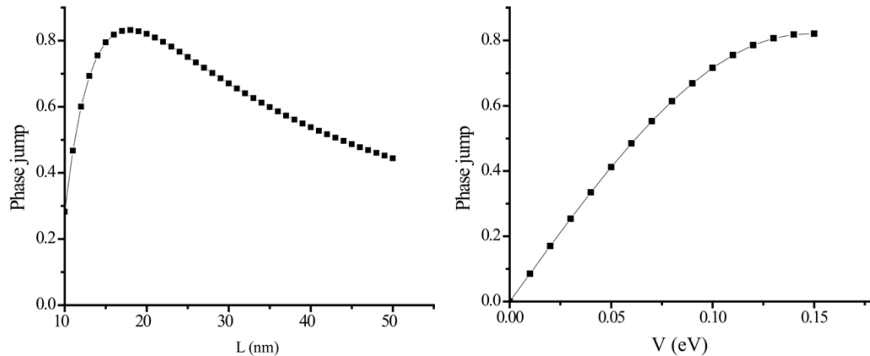


Figure 4: Displays the magnitude of the phase jump corresponding to the Berry phase in the population distribution of CB states of graphene superlattice as a function of (a) moiré wavelength (L) in nanometer, and (b) potential strength (V) in electron volt.

terference fringes predicted in this Letter and their evolution caused by electron collisions.

In Fig. 4, we plot the magnitude of jump in CB distribution associated with the Berry phase as a function of moiré wavelength (λ) and potential strength (V). The magnitude of the jump has been scaled between 0 and 1, corresponding to the phase difference of 0 to π . The phase jump as a function of moiré wavelength exhibits a maximum at around 20 nm which predicts the optimum value gating length. On the other hand, the magnitude of the Berry phase jump displays a monotonic behavior with respect to the gating potential before it reaches a plateau at $V \sim 0.15\text{eV}$.

4. CONCLUSION

We present a developmental study of our preceding letter [25] where we looked into the self-referenced interferometry in pristine graphene with the use of few-cycle circularly polarized pulse to detect the non-trivial Berry phase of $\pm\pi$ corresponding to electron trajectories encircling the K - and K' - points. Although the characteristics of non-trivial Berry curvature of graphene was evident in the chiral structure of electron distribution in CB and the formation of bifurcation, the direct visualization of the phase shift corresponding to the π -phase was out of sight of the tr-ARPES eye. We overcome this subtlety by overlaying graphene on a hexagonal Boron Nitride (h-BN) substrate and making a superlattice moiré pattern. Due to the Bragg reflection caused by this extra weak (and periodic) interlayer potential, states with different crystallographic wave vectors couple with each other and thereby reduce the Berry phase to less than a full period. Such a reduced symmetry system manifests the Berry phase as discontinuities

on the interferometric distribution of electrons and thereafter can be read out using attosecond pulses produced by high harmonic generation. Berry phase as the phase factor of electron wave function contains rich information about the singular nature of the Dirac cones and the chirality of graphene and hence of great importance in understanding the band theory of solids and their intrinsic topological essence, as well as emerging phenomena like Valleytronics, quantum Hall effects, and topological superconductivity.

APPENDIX A: DESCRIPTION OF BERRY PHASE WITHIN TOPOLOGICAL BAND THEORY OF GRAPHENE

Revealing the electronic band structure of graphene over the entire Brillouin zone in the electric field of the pulse requires a lattice description of the system. Knowing the band structure properties for the whole Brillouin zone allows us to calculate the relevant topological quantum numbers and identify the topological (Berry) phase of the graphene system. From the definition, the interband dipole elements are calculated as below:

$$D_x = \frac{V_x}{i(E_c - E_v)/\hbar} = \frac{1}{i(E_c - E_v)} \langle v | \frac{\partial H}{\partial k_x} | c \rangle \quad (\text{A1})$$

Where

$$\langle v | \frac{\partial H}{\partial k_x} | c \rangle = \frac{\partial}{\partial k_x} (\langle v | H | c \rangle) - \langle \partial_{k_x} v | H | c \rangle - \langle v | H | \partial_{k_x} c \rangle = (E_c - E_v) \langle v | \partial_{k_x} c \rangle \quad (\text{A2})$$

Using the following identity

$$\partial_{k_x} \langle v | c \rangle = 0 = \langle \partial_{k_x} v | c \rangle + \langle v | \partial_{k_x} c \rangle \quad (\text{A3})$$

we get the following expression for D_x as:

$$D_x = \frac{1}{i} \langle v | \partial_{k_x} c \rangle \quad (\text{A4})$$

By definition, the Berry phase is given by the following expression

$$\theta = -i \oint_c \langle c | \partial_t | c \rangle dt \quad (\text{A5})$$

Without loss of generality, we can assume a particular loop in reciprocal space around the Dirac point that the change in k_y is negligible. Hence, the Berry phase can be rewritten as below:

$$\theta = -i \left[\underbrace{\int_{-a}^a \langle c | \partial_{k_x} c \rangle dk_x}_{K_y+0} + \underbrace{\int_a^{-a} \langle c | \partial_{k_x} c \rangle dk_x}_{K_y-0} \right] \quad (\text{A6})$$

The integrand of the above integral is equal to:

$$\langle c | \partial_{k_x} c \rangle = \langle c | \frac{1}{\sqrt{2}} \left(i e^{i\phi} \frac{\partial \phi}{\partial k_x} \right) e^{ikr} + \frac{1}{\sqrt{2}} (e^1) | e^{ikr} x \rangle = \frac{i}{2} \frac{\partial \phi}{\partial k_x} \quad (\text{A7})$$

Similarly one can obtain:

$$\langle v | \partial_{k_x} c \rangle = -\frac{i}{2} \frac{\partial \phi}{\partial k_x} \quad (\text{A8})$$

Hence,

$$\langle c | \partial_{k_x} c \rangle = -\langle v | \partial_{k_x} c \rangle = -i D_x \quad (\text{A9})$$

Substituting Eq. (A9) into Eq. (A6) reads:

$$-i \left[\underbrace{i \int_{-a}^a D_x dk_x}_{K_y=0} - i \underbrace{\int_{-a}^a D_x dk_x}_{K_y+0} \right] = \underbrace{\int_{-a}^a D_x dk_x}_{K_y=0} - \underbrace{\int_{-a}^a D_x dk_x}_{K_y+0} = \pi = \theta \quad (\text{A10})$$

REFERENCES

- [1] A. Schiffrin, T. Paasch-Colberg, N. Karpowicz, V. Apalkov, D. Gerster, S. Muhlbrandt, et al., "Optical-field-induced current in dielectrics," *Nature*, vol. 493, pp. 70-4, Jan 32013.
- [2] M. Schultze, E. M. Bothschafter, A. Sommer, S. Holzner, W. Schweinberger, M. Fiess, et al., "Controlling dielectrics with the electric field of light," *Nature*, vol. 493, pp. 75-8, Jan 32013.
- [3] F. Krausz and M. I. Stockman, "Attosecond metrology: from electron capture to future signal processing," *Nat Photon*, vol. 8, pp. 205-213, 03//print 2014.
- [4] M. Schultze, K. Ramasesha, C. D. Pemmaraju, S. A. Sato, D. Whitmore, A. Gandman, et al., "Attosecond bandgap dynamics in silicon," *Science*, vol. 346, pp. 1348-1352, December 12, 2014.
- [5] G. Vampa, T. J. Hammond, N. Thiré, B. E. Schmidt, F. Légaré, C. R. McDonald, et al., "All-Optical Reconstruction of Crystal Band Structure," *Physical Review Letters*, vol. 115, p. 193603, 11/05/ 2015.
- [6] H. K. Kelardeh, M. I. Stockman, and V. Apalkov, "Buckled Dirac Materials in Ultrashort and Strong Optical Field: Coherent Control and Reversibility Modulation," *IEEE Transactions on Nanotechnology*, vol. 15, pp. 51-59, jan 2016.
- [7] M. F. Ciappina, J. A. Pérez-Hernández, A. S. Landsman, W. A. Okell, S. Zherebtsov, B. Förg, et al., "Attosecond physics at the nanoscale," *Reports on Progress in Physics*, vol. 80, p. 054401, 2017.
- [8] M. V. Berry, "Quantal Phase Factors Accompanying Adiabatic Changes,"

- Proceedings of the Royal Society of London A: Mathematical, Physical and Engineering Sciences, vol. 392, pp. 45-57, 1984-03-08 00:00:00 1984.
- [9] D. Xiao, M.-C. Chang, and Q. Niu, "Berry phase effects on electronic properties," *Reviews of Modern Physics*, vol. 82, pp. 1959-2007, 07/06/ 2010.
- [10] G. P. Mikitik and Y. V. Sharlai, "Manifestation of Berry's Phase in Metal Physics," *Physical Review Letters*, vol. 82, pp. 2147-2150, 03/08/ 1999.
- [11] N. Nagaosa, J. Sinova, S. Onoda, A. H. MacDonald, and N. P. Ong, "Anomalous Hall effect," *Reviews of Modern Physics*, vol. 82, pp. 1539-1592, 05/13/ 2010.
- [12] D. J. Thouless, M. Kohmoto, M. P. Nightingale, and M. den Nijs, "Quantized Hall Conductance in a TwoDimensional Periodic Potential," *Physical Review Letters*, vol. 49, pp. 405-408, 08/09/ 1982.
- [13] M. Z. Hasan and C. L. Kane, "\textit{Colloquium} : Topological insulators," *Reviews of Modern Physics*, vol. 82, pp. 3045-3067, 11/08/ 2010.
- [14] K. I. Bolotin, K. J. Sikes, Z. Jiang, M. Klima, G. Fudenberg, J. Hone, et al., "Ultrahigh electron mobility in suspended graphene," *Solid State Communications*, vol. 146, pp. 351-355, 2008/06/01/ 2008.
- [15] L. Wang, I. Meric, P. Y. Huang, Q. Gao, Y. Gao, H. Tran, et al., "One-Dimensional Electrical Contact to a Two-Dimensional Material," *Science*, vol. 342, pp. 614-617, 2013-11-01 00:00:00 2013.
- [16] J. Wang, Y. Hernandez, M. Lotya, J. N. Coleman, and W. J. Blau, "Broadband Nonlinear Optical Response of Graphene Dispersions," *Advanced Materials*, vol. 21, pp. 2430-2435, 2009.
- [17] S. A. Mikhailov, "Non-linear electromagnetic response of graphene," *EPL (Europhysics Letters)*, vol. 79, p. 27002, 2007.
- [18] H. K. Kelardeh, V. Apalkov, and M. I. Stockman, "Graphene in ultrafast and superstrong laser fields," *Physical Review B*, vol. 91, p. 045439, 2015.
- [19] M. T. Hassan, T. T. Luu, A. Moulet, O. Raskazovskaya, P. Zhokhov, M. Garg, et al., "Optical attosecond pulses and tracking the nonlinear response of bound electrons," *Nature*, vol. 530, pp. 66-70, 02/04/print 2016.
- [20] E. I. Blount, "Bloch Electrons in a Magnetic Field," *Physical Review*, vol. 126, pp. 1636-1653, 06/01/ 1962.
- [21] Y. Zhang, Y.-W. Tan, H. L. Stormer, and P. Kim, "Experimental observation of the quantum Hall effect and Berry's phase in graphene," *Nature*, vol. 438, pp. 201-204, 11/10/print 2005.
- [22] K. S. Novoselov, E. McCann, S. V. Morozov, V. I. Fal'ko, M. I. Katsnelson, U. Zeitler, et al., "Unconventional quantum Hall effect and Berry's phase of 2π in bilayer graphene," *Nat Phys*, vol. 2, pp. 177-180, 03/print 2006.
- [23] C. Hwang, C.-H. Park, D. A. Siegel, A. V. Fedorov, S. G. Louie, and A. Lanzara, "Direct measurement of quantum phases in graphene via photoemission spectroscopy," *Physical Review B*, vol. 84, p. 125422, 09/09/ 2011.
- [24] Y. Liu, G. Bian, T. Miller, and T. C. Chiang, "Visualizing Electronic Chirality and Berry Phases in Graphene Systems Using Photoemission with Circularly Polarized Light," *Physical Review Letters*, vol. 107, p. 166803, 10/10/ 2011.
- [25] H. K. Kelardeh, V. Apalkov, and M. I. Stockman, "Attosecond strong-field interferometry in graphene: Chirality, singularity, and Berry phase," *Physical*

- Review B, vol. 93, p. 155434, 04/26/ 2016.
- [26] M. Yankowitz, J. Xue, D. Cormode, J. D. Sanchez-Yamagishi, K. Watanabe, T. Taniguchi, et al., "Emergence of superlattice Dirac points in graphene on hexagonal boron nitride," *Nat Phys*, vol. 8, pp. 382-386, 05//print 2012.
- [27] L. A. Ponomarenko, R. V. Gorbachev, G. L. Yu, D. C. Elias, R. Jalil, A. A. Patel, et al., "Cloning of Dirac fermions in graphene superlattices," *Nature*, vol. 497, pp. 594-597, 05/30/print 2013.
- [28] R. V. Gorbachev, J. C. W. Song, G. L. Yu, A. V. Kretinin, F. Withers, Y. Cao, et al., "Detecting topological currents in graphene superlattices," *Science*, vol. 346, p. 448, 2014.
- [29] J. C. W. Song, P. Samutpraphoot, and L. S. Levitov, "Topological Bloch bands in graphene superlattices," *Proceedings of the National Academy of Sciences*, vol. 112, pp. 10879-10883, September 1, 20152015.
- [30] L. Wang, Y. Gao, B. Wen, Z. Han, T. Taniguchi, K. Watanabe, et al., "Evidence for a fractional fractal quantum Hall effect in graphene superlattices," *Science*, vol. 350, pp. 1231-1234, 2015-12-04 00:00:00 2015.
- [31] H. K. Keldar, V. Apalkov, and M. I. Stockman, "Graphene superlattices in strong circularly polarized fields: Chirality, Berry phase, and attosecond dynamics," *Physical Review B*, vol. 96, Aug 72017.
- [32] A. N. Grigorenko, M. Polini, and K. S. Novoselov, "Graphene plasmonics," *Nat Photon*, vol. 6, pp. 749-758, 11//print 2012.
- [33] J. C. Johannsen, S. Ulstrup, F. Cilento, A. Crepaldi, M. Zacchigna, C. Cacho, et al., "Direct View of Hot Carrier Dynamics in Graphene," *Physical Review Letters*, vol. 111, p. 027403, 07/09/ 2013.
- [34] I. Gierz, J. C. Petersen, M. Mitrano, C. Cacho, I. C. Turcu, E. Springate, et al., "Snapshots of non-equilibrium Dirac carrier distributions in graphene," *Nat Mater*, vol. 12, pp. 1119-24, Dec 2013.
- [35] M. W. Graham, S.-F. Shi, D. C. Ralph, J. Park, and P. L. McEuen, "Photocurrent measurements of supercollision cooling in graphene," *Nat Phys*, vol. 9, pp. 103-108, 02//print 2013.
- [36] D. Brida, A. Tomadin, C. Manzoni, Y. J. Kim, A. Lombardo, S. Milana, et al., "Ultrafast collinear scattering and carrier multiplication in graphene," *Nat Commun*, vol. 4, 06/17/online 2013.
- [37] M. Breusing, S. Kuehn, T. Winzer, E. Malić, F. Milde, N. Severin, et al., "Ultrafast nonequilibrium carrier dynamics in a single graphene layer," *Physical Review B*, vol. 83, p. 153410, 04/19/ 2011.
- [38] S. Das Sarma, S. Adam, E. H. Hwang, and E. Rossi, "Electronic transport in two-dimensional graphene," *Reviews of Modern Physics*, vol. 83, pp. 407-470, 05/16/ 2011.
- [39] K. J. Tielrooij, J. C. W. Song, S. A. Jensen, A. Centeno, A. Pesquera, A. Zurutuza Elorza, et al., "Photoexcitation cascade and multiple hot-carrier generation in graphene," *Nat Phys*, vol. 9, pp. 248-252, 04//print 2013.
- [40] E. Malic, T. Winzer, E. Bobkin, and A. Knorr, "Microscopic theory of absorption and ultrafast many-particle kinetics in graphene," *Physical Review B*, vol. 84, p. 205406, 11/10/ 2011.
- [41] H. K. Keldar, V. Apalkov, and M. I. Stockman, "Wannier-Stark states of

- graphene in strong electric field," *Physical Review B*, vol. 90, p. 085313, Aug 28 2014.
- [42] H. K. Kelardeh and M. I. Stockman, "Theoretical study of electron dynamics in graphene interacting with ultrafast and ultrastrong laser pulses," in *SoutheastCon 2015*, 2015, pp. 1-5.
- [43] D. Pesin and A. H. MacDonald, "Spintronics and pseudospintronics in graphene and topological insulators," *Nat Mater*, vol. 11, pp. 409-416, 05//print 2012.
- [44] W. V. Houston, "Acceleration of Electrons in a Crystal Lattice," *Physical Review*, vol. 57, pp. 184-186, 02/01/ 1940.
- [45] H. K. Kelardeh, V. Apalkov, and M. I. Stockman, "Graphene under a few-cycle circularly polarized optical field: ultrafast interferometry and Berry phase manifestation," in *SPIE Nanoscience + Engineering*, 2016, pp. 99320E-99320E-9.
- [46] M. B. Lundberg and J. A. Folk, "Harnessing chirality for valleytronics," *Science*, vol. 346, p. 422, 2014.
- [47] J. R. Schaibley, H. Yu, G. Clark, P. Rivera, J. S. Ross, K. L. Seyler, et al., "Valleytronics in 2D materials," *Nature Reviews Materials*, vol. 1, p. 16055, 08/23/online 2016.
- [48] Y. Aharonov and D. Bohm, "Significance of Electromagnetic Potentials in the Quantum Theory," *Physical Review*, vol. 115, pp. 485-491, 08/01/ 1959.
- [49] A. Damascelli, Z. Hussain, and Z.-X. Shen, "Angle-resolved photoemission studies of the cuprate superconductors," *Reviews of Modern Physics*, vol. 75, pp. 473-541, 04/17/ 2003.
- [50] J. Avila, I. Razado, S. Lorcy, R. Fleurier, E. Pichonat, D. Vignaud, et al., "Exploring electronic structure of oneatom thick polycrystalline graphene films: A nano angle resolved photoemission study," *Scientific Reports*, vol. 3, p. 2439, 08/14/online 2013.